Atomic force microscopy combined with human pluripotent stem cell derived cardiomyocytes for biomechanical sensing

Martin Pesl, Jan Pribyl, Ivana Acimovic, Aleksandra Vilotic, Sarka Jelinkova, Anton Salykin, Alain Lacampagne, Petr Dvorak, Albano C Meli, Petr Skladal, et al.

Atomic force microscopy combined with human pluripotent stem cell derived cardiomyocytes for biomechanical sensing

Martin Pesl [a,b,1], Jan Pribyl [c,1], Ivana Acimovic [a], Aleksandra Vilotic [a], Sarka Jelinkova [a], Anton Salykin [a,b], Alain Lacampagne [d], Petr Dvorak [a,b], Albano C. Meli [a,d], Petr Skladal [c,*], Vladimir Rotrekl [a,b]

[a] Department of Biology, Faculty of Medicine, Masaryk University, Brno, Czech Republic
[b] ICRC, St. Anne's University Hospital, Brno, Czech Republic
[c] CEITEC, Masaryk University, Brno, Czech Republic
[d] PhyMedExp, INSERM U1046, University of Montpellier, Montpellier, France

Keywords:
Micromechanical biosensor
Human stem cell
Cardiomyocyte contraction
Drug testing

A B S T R A C T

Cardiomyocyte contraction and relaxation are important parameters of cardiac function altered in many heart pathologies. Biosensing of these parameters represents an important tool in drug development and disease modeling. Human embryonic stem cells and especially patient specific induced pluripotent stem cell-derived cardiomyocytes are well established as cardiac disease model.. Here, a live stem cell derived embryoid body (EB) based cardiac cell syncytium served as a biorecognition element coupled to the microcantilever probe from atomic force microscope thus providing reliable micromechanical cellular biosensor suitable for whole-day testing.

The biosensor was optimized regarding the type of cantilever, temperature and exchange of media; in combination with standardized protocol, it allowed testing of compounds and conditions affecting the biomechanical properties of EB. The studied effectors included calcium , drugs modulating the catecholaminergic fight-or-flight stress response such as the beta-adrenergic blocker metoprolol and the beta-adrenergic agonist isoproterenol. Arrhythmogenic effects were studied using caffeine. Furthermore, with EBs originating from patient's stem cells, this biosensor can help to characterize heart diseases such as dystrophies.

1. Introduction

Cell based biosensor (CBB) devices represent a novel tool to understand and treat various human diseases including heart diseases which are leading cause of death in developed countries (Pilkerton et al., 2015). Most of them have hidden cause at the cellular and genetic levels (Aistrup et al., 2009; Stienen, 2015) not easily accessible for diagnostics, as heart biopsy is invasive procedure with significant risk (Holzmann et al., 2008; Imamura et al., 2015). Since the discovery of pluripotent stem cells (PSCs), such as human embryonic stem cells (hESC) (Thomson et al., 1998) and especially disease specific induced pluripotent stem cells (hiPSC) (Takahashi et al., 2007) and their differentiation into cardiomyocytes (Mummery et al., 2002), these cell types represent an important cellular model in drug and disease screening (reviewed in Acimovic et al., 2014).

The electrophysiological phenotype of individual cardiac cells is often studied providing information representing pacemaker or messenger function. Despite most of studies use single cells, the CMs syncytium seems to be a critical parameter in biosensor assembly as unstable signals are obtained in case of individual or small cluster of cells (Kaneko et al., 2007, 2014). These methods follow mostly action potential, cell to cell conductivity or electrical cell-substrate impedance (Giaever and Keese, 1984). Recently, xCELLigence RTCA Cardio multiwell sensor combined with primary neonatal rat cells was used to monitor the effect of antiarrhythmic drugs on cell growth and contractions (Guo et al., 2011). However, the electrophysiological data cannot be fully separated from the mechanical triggers and consequences (Kelly et al., 2006) rendering the method not suitable for large group of diseases affecting electro-mechanical coupling. Thus CM contraction and relaxation biosensing represents an indispensable step for the in vitro disease modeling. Indirect methods of contraction measurement, such as optical ones based on optical fiber deformation (Fearn et al., 1993) and image analysis (Neagoe et al., 2003) have limited potential especially in case of in vitro differentiated CMs,

* Correspondence to: Department of Biochemistry, Masaryk University, Kamenice 5, CZ-62500 Brno, Czech Republic.
E-mail address: skladal@chemi.muni.cz (P. Skladal).
[1] These authors contributed equally to this work.

which do not fully match the shape of the isolated CMs and often require dissociation of the syncytium and analyzing the individual cells in microposts (Rodriguez et al., 2014). Furthermore, the combination of optical analysis and the direct methods measuring contraction force on artificially assembled structures are significantly impacted by stiffness of the substrate, such as the twitch power in the case of dissociated cells plated on substrate with varying stiffness (Rodriguez et al., 2011). Further the increasing cell number negatively impacted the force-length relationship measured directly on neonatal cardiac cells self-assembled on fibrin fibers (Sondergaard et al., 2012), again rendering the syncytium analysis at least difficult. Thus it seems that the most promising structure for studying the contraction properties of human cardiac syncytium might be uniformly sized clusters of differentiated CMs in the form of PSCs-derived embryoid bodies (Pesl et al., 2014). Therefore we opted for a direct approach to assess the EBs' cardiac syncytium mechanical properties in real time and under the alternating biophysical and biochemical conditions using atomic force microscopy (AFM).

AFM is a three-dimensional high resolution topographic technique. It is suitable for biological applications in native conditions (Vahabi et al., 2013) with the ability to measure bending of the cantilever probe with extremely high precision (Sundararajan and Bhushan, 2002). It allows AFM to be used as a mechanical nanosensor (Wang et al., 2015), or as a micromechanical transducer for the construction of biosensors (Lavrik et al., 2004). Furthermore, modified AFM tip biosensor has been used in numerous studies, including the analysis of Alzheimer's disease process (Hane et al., 2014), as mechanical sensor in the study of cell penetration by nanoneedles (Obataya et al., 2005), in cell-based biosensing of drug effects (Wang et al., 2009) and in study of growth factor effects on epidermal cells (Zhang et al., 2014).

In this study, our previously developed uniformly sized EBs containing human induced pluripotent stem cell-derived cardiomyocytes (hiPSC-CMs) (Pesl et al., 2014) are integrated into the AFM force sensing platform to perform a high fidelity contraction pattern as a unique CBB for the measurement of absolute values of contractile forces together with frequency of the beat rate in complex conditions and cellular models. Development and optimization of the whole measurement setup is described with proposed application for characterization of cell clusters of cardiac cells and testing effects of model drugs.

2. Materials and methods

2.1. Preparation of hiPSC and hESC cardiomyocyte clusters

Measurements were performed using the hESC lines CCTL14 and CCTL12, characterized previously (Dvorak et al., 2005; International Stem Cell Initiative et al., 2007; Krutá et al., 2013). The hiPSC line cl1 was obtained from Dr. Majlinda Lako, Institute of Genetic Medicine, Newcastle University and the iPSC lines MDMD2Se were derived in our laboratory from human skin biopsies (Krutá et al. 2014). The hESCs and iPSC lines were propagated on mitotically inactivated mouse embryonic fibroblasts (Dvorak et al., 2005). Regular round shape of embryoid bodies was achieved by forced aggregation in silicone mold preformed microwells (1.5% agarose, VWR) (Dahlmann et al., 2013), their differentiation and maturation was achieved using our previously described method (Pesl et al., 2014). For statin samples, PSC were cultivated with pravastatin (20 μM, Sigma) for 4 days prior to EB formation.

2.2. Clusters seeding and measurement set-up

Beating EBs cultured for 28 days after initiation of differentiation were selected for round shape and adequate size and seeded onto adherent 30 mm Petri dishes (TPP Technoplastic Products, Trasadingen, Switzerland). The cultivation media was replaced by Tyrod solution (135 mM NaCl, 10 mM HEPES, 5.4 mM KCl, 0.9 mM $MgCl_2$, pH 7.4) and suplemented with 10 mM glucose and $CaCl_2$ (in desired concentration) and the EBs were maintained at 37 °C in a standard CO_2 incubator. Before experiment, a dish equipped with media exchange tubes was placed on the motorized stage of an inverted microscope (Olympus IX-81S1F-3, Tokyo, Japan) and the AFM recording head (BioAFM NanoWizard 3, JPK, Berlin, Germany) was finally placed on top of the sample. The AFM set-up was modified in order to provide real-time biomechanical characterization of CMs cell clusters (Fig. 1).

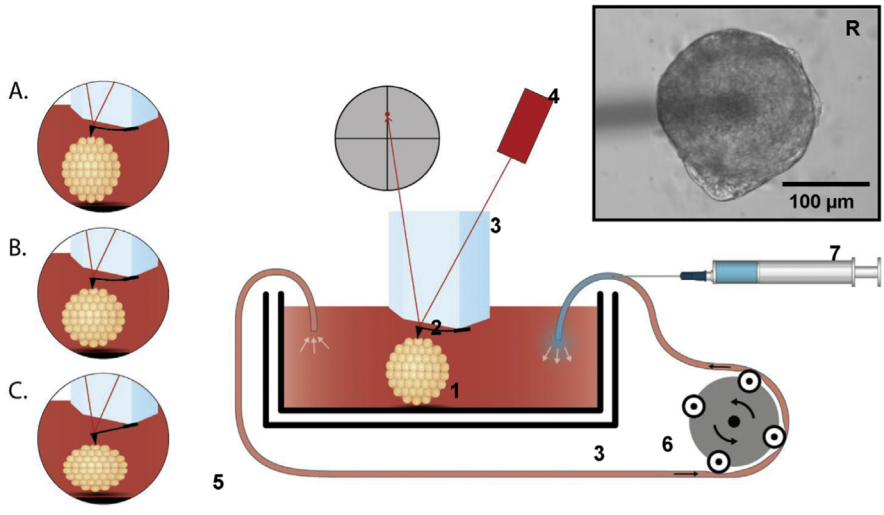

Fig. 1. Scheme of the biosensor setup used for biomechanical characterization of cardiomyocyte clusters. Most important parts are schematically shown and are labeled as follows: 1 – Embryonic body (EB, cluster of living cells) in plastic Petri dish, (3 cm in diameter), 2 – AFM cantilever, equipped with a sharp tip, 3 – glass cantilever holder block, 4 – AFM laser source (a) (left) and photodetector of laser (b), position, 5 – plastic (PP) tubing, i.d. 0.2 mm (an arrow shows the flow direction), 6 – peristaltic pump, driving the flow direction and rate (rotation direction is shown by an arrow), 7 – medical syringe (total volume of 1.0 ml) for drug injection, 8 – Petri dish heater (to keep constant temperature of 37.0 ± 0.1 °C). The little insets on the left (A, B and C) show the subsequent stages of the EB contractile movement as this is measured by the AFM cantilever. Image (R) in the top-right corner shows real image of EB cluster with cantilever on its surface (captured by optical microscope). The size of the EB cluster is 175 μm.

The cantilever glass holder placed on the AFM head (scanning by probe, range in X-Y-Z was 100–100–15 μm) was equipped with soft cantilever and the contact part of the head was submersed in the 30 mm Petri dish containing one or more EBs at the bottom of non-treated plastic. The Petri dish heater (JPK, Berlin, Germany) was used to either keep the temperature constant at 37 °C or at 29–37 °C for temperature dependency studies. Scanning probe microscope (SPM) Control Software v.4 (JPK) was used for instrument control and data acquisition at 1 kHz rate. For further details, see part 1.1 of Supplementary Material (SM).

2.3. Recording of mechanocardiograms

The mechanocardiogram (MCG) curve shows the interaction force between the AFM tip and the surface of the beating cells cluster recorded in a real time. The force between the AFM probe and the studied surface was kept constant as defined by the set point (SP) value, carried out by the feedback loop. Intensity of feedback is given by integral and proportional gain parameters (IGain/PGain). The various AFM cantilever probes used are described in the supplementary materia (SM) part 2.3.

In order to determine the effect of the set point value on the measured force (MCG curves), the cantilever (Hydra-6R, AppNano, Mountain View, CA, USA) was left to land onto the beating CM cell cluster stabilized for 15 min at 37 °C. The MCGs were recorded in 10 min intervals using SP set to 0, 1, 3, 6, 9, 12, 15 and 18 nN (whole measuring range of the biosensor setup given by stiffness and sensitivity), where the SP=0 value means operation in the so called passive mode, i.e. it does not follow the cell movement (zero interaction force) and only the living beating cell cluster is leveling the cantilever, similar as in the literature (Liu et al., 2012).

The effect of temperature stability on MCG recording and behavior of CM clusters at different temperatures are provided in SM parts 2.4 and 2.5, respectively. The protocol for studying effect of different concentration of calcium is given in the SM part 2.6.

2.4. Surface homogeneity of the biomechanical properties

EB is a spherical cluster (300 μm in diameter) consisting of approximately 2000 cells; fluorescent images of EB are provided in Fig. S1. In order to map the homogeneity of the beating force on the surface of the CMs cluster, nine points of the surface of the cell cluster were screened (scheme included in Fig. 3). The uncoated silicon nitride cantilever Hydra-6R-200N (AppNano), characterized by spring constant of 0.025 N/m and sensitivity 10.1 nm/V was used. Motorized stage of the AFM microscope was used to move the AFM probe between the positions, when the Z-driving piezo was in the retracted state and the probe was 50 μm above the cell surface. When in place, AFM cantilever was landed onto the beating cell cluster of cardiomyocytes (EB), preheated and stabilized. The MCG curve was recorded for 10 min in each position with constant set point value of 6 nN. 5 min recordings of MCG curves were evaluated for the force and beat rate comparison.

2.5. Evaluation of signal traces

Time-series data saved from the Nanowizard AFM were preprocessed and analyzed by in-house developed algorithm using MATLAB 2015a (ver. 8.5, The MathWorks Inc., Natick, USA). After resampling (noise and dataset size reduction), the local maximum and its corresponding local minimum for each contraction were identified and processed to obtain the force of each individual contraction (R-S amplitude) and beat rate of EB. The Mann-Whitney's *U*-test was used to evaluate two group comparisons.

2.6. Statistical evaluation of data

Quantitative data are presented as the mean ± the standard error of the mean from 3 to 6 experiments (indicated as *N* in the appropriate graph). The normality of data distribution was evaluated by the Shapiro-Wilk method thus proving the data normality at the 0.05 level. One way Student's *t*-test was used to test statistical difference of the measured data sets at the level 0.05 (maps of force on the cell cluster) when they were compared to the mean value. One way ANOVA method implementing the Bonferroni test was employed to compare statistical significance of measured signals (force/beat rate) at different concentrations of calcium, significance was compared either at different levels ($p < 0.05$, $p < 0.01$, $p < 0.005$) or was calculated as value. Microcal Origin 7.0 software (Microcal, Northampton, MA, USA was used for statistical processing of the data.

3. Results and discussion

3.1. Cardiomyocyte cluster biosensor construction

The multicellular biosensor device was constructed by implementing the embryoid body inside the AFM measurement chamber as shown in Fig. 1. The major difference compared to previously reported approach (Liu et al., 2012) was the use of the embryoid body as multicellular syncytium rather than individual cardiomyocytes. EBs were characterized by immunofluorescence using anti α-actinin antibody and DAPI staining (Fig. S1A), providing distribution of cardiomyocytes within the syncytium. After dissociating the beating EB into individual cells, the obtained DAPI/α-actinin and DAPI/cardiac troponin T fluorescence patterns (Fig. 1SB) were as expected for mature cardiomyocytes.

The use of the cluster of CMs seems to be a significant advantage regarding robustness of the resulting system. Typically, the CMs-based biosensing experiments were running successfully for up to 8 h. A fresh sterile medium was exchanged when needed, however, the experiments were otherwise carried out in non-sterile conditions inside the acoustic isolation chamber containing the microscopes. The AFM cantilever contacting surface of the cell cluster was kept fixed in the horizontal plane and the contraction force was monitored in real time by the vertical bending of the cantilever. Other parameters such as beating frequency and kinetics of the responses were precisely determined by the data post-processing.

The effect of various set point values on the AFM biosensor with the CMs-based EB was tested. The force and "heart" beat rate (BR) of the EB were recorded (Fig. 2A) while the set point value was gradually increased from 1 nN up to 18 nN (Fig. 2B). The BR values did not differ significantly within the tested range demonstrating robustness of the biosensor set-up and also suggesting that the force application does not lead to BR changes due to the activation of mechano-sensitive ion channels normally present in cardiomyocytes. Interestingly, the initial significant and steep increase in contraction force between the set point 0 and 5 nN was observed. The explanation for the initial ramp below 5 nN is demonstrated by the curves of force measured with 3 different values of set point (0, 6 and 10 nN) shown in Fig. 2A.

The curve measured with SP=0 nN (passive mode) is missing the feedback loop resulting from the EB relaxation rendering the data incomplete. Application of 6 nN of SP force to the cantilever resulted in recording complete dataset of force needed to compensate the EB cluster movement. Thus, the active mode was preferred to the passive one (Liu et al., 2012), possibly due to the limited mechanical integrity of dissociated CMs on the non elastic surface. Further increase in SP force to 10 nN led to subsequent

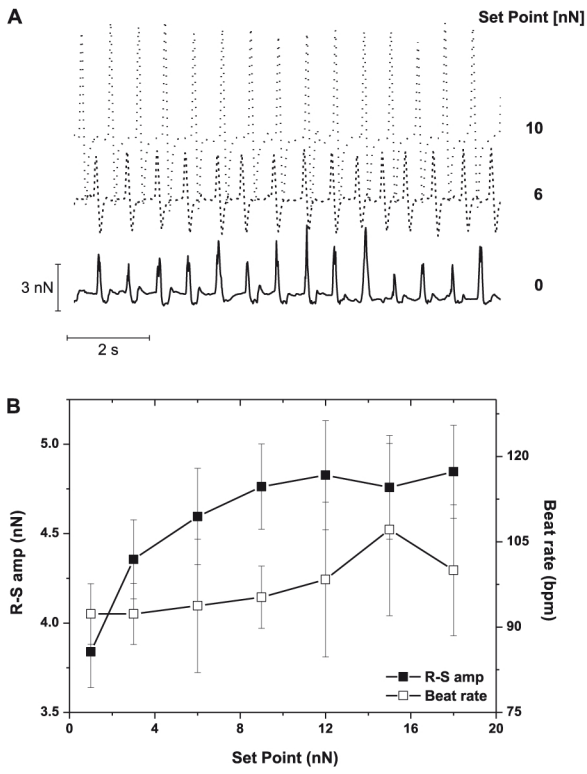

Fig. 2. A Comparison of real time curves recorded during the passive (set point value 0 nN) and active mode, with two different values of set point. B Effect of set point value on force (*r*-S amp) and beat rate of EB. Average of median values is shown in the graph, error bars are equal to standard deviation of values, N=2.

insignificant increase in contraction force; however this, based on the curve shape (Fig. 2(A)), can be explained by mechanical stimulation of the cells in the cluster and activation of mechanosensitive ion channels (e.g. Lin et al., 2007) rather than by inability to record full contraction with SP=6 nN as in case of the passive mode (0 nN).

Therefore, the optimal value of set point for experiments was set at 6 nN, this is also close to the average values of EBs contraction forces. Such set point force allows for the measurement of 95% of maximum contraction force (4.6 nN vs. 4.85 nN, when SP was 6 and 18 nN, respectively), with no effect on BR therefore minimizing the effect of the mechanical stimulation. On the other hand, further increase in SP force, stimulating the mechano-sensitive ion channels and/or adherens junctions present in the syncytium, enables the EB containing biosensor to be useful for modeling and/or drug screening in case of hypertension and stretch related hypertrophy (Yamazaki et al., 1998) or cardiac injury related tension changes between myocyte and fibroblast (Thompson et al., 2011).

3.2. *Biomechanical properties are homogenous on the EB surface*

The effect of localization of the AFM probe on the surface of the cell cluster was tested; the measuring position ideally should not significantly influence the resulting biomechanical parameters. Nine points homogenously located on the EB surface were chosen (Fig. 3) and the contraction force and BR were determined. Furthermore, to evaluate potential influence of the EB phenotype, these experiments were repeated for three different types of EBs including normal control EBs generated under hypoxic conditions (Hypoxia), disease model EBs with pathologicaly affected

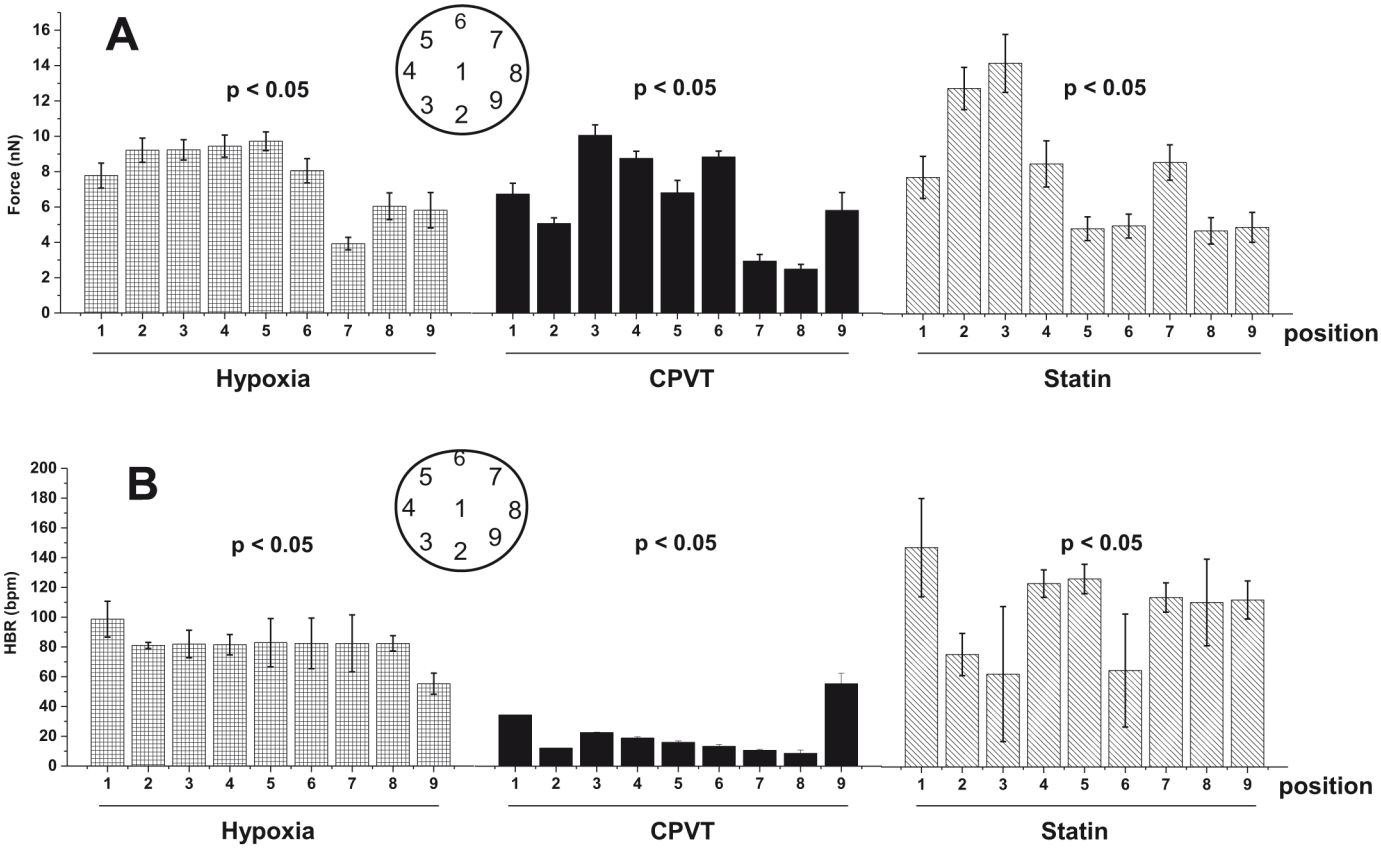

Fig. 3. Mapping of the force on the surface of the EB cluster. Average of median values of beating force (A) and beat rate (B) recorded in different positions on cell cluster surface are presented in the graphs as data sets (groups) of values measured for every cell cluster. Map of positions on EB surface is shown in the upper part of both graphs., error bars are equal to standard deviation of values, N=3. The data normality was confirmed by Shapiro Wilk test at 0.05 level. All the data sets were found not to be significantly different from the mean value at the same level (0.05), as indicated in the graph.

excitation-contraction coupling (CPVT) (Meli et al., 2011 and unpublished data), and EBs derived from the cells treated with statins (Jelinkova et al., unpublished).

Consistent values of the contraction force and beating frequency were found by screening of a single EB across the nine detection points and even the EB-to-EB values covered quite narrow interval (Fig. 3; the detailed statistical values are included as Table S1 in SM). However, the contraction force variability on peripheral detection points implicates some positional effect and possibly the effect of biomagnetic fields produced by the EB's electric activity and stresses the importance to choose the detection point with highest response for further analysis. The highest reproducibility was observed for the normal (Hypoxia) EBs. The minor effect of the exact positioning of the microcantilever probe at biosurface seems to be the most important advantage of the cluster of (several hundredths) cells compared to experiments carried out on individual cardiomyocytes. Single cells either separately adhering to the surface or as part of the two-dimensional layer are typically much more affected by the contacting cantilever, and if present, the sharp tip might damage the cell membrane. In the case of cell cluster, damage of few surface-located cells contacting the probe is not very significant. From the practical point of view, this is quite significant advantage of the cluster of cells serving as the biorecognition element.

3.3. Effect of temperature on the cardiomyocytes-based biosensor

Temperature affects the beat rate as well as arrhytmogenic cardiomyocyte potential (Chen et al., 2003). Furthermore, temperature affects also stability of the cantilever and its coupling with EB in the biosensor set-up. Contrary to the desired effect of temperature on the cardiomyocyte function (biorecognition process), its effect on the stability of the transducer system should be eliminated by choosing suitable components and optimal conditions.

To characterize the effect of cantilever type and its temperature instability independent of the EB activity, live but non beating EB coupled with variety of AFM probes were evaluated between 30 and 37 °C; details are discussed in SM and shown in Fig. S2. The instability usually results from the bimetallic effect combined with adsorption events on the hydrophobic surface of the coating metal layer (Samori, 2009). Thus, the uncoated silicon nitride cantilever (HYDRA-6R, pyramidal tip) provided most stable force reading and higher reflection of laser beam comparing to the tip-less version (HYDRA TL). Gold-coated SNL-10 probe exhibited the highest variability in the force signal, suggesting limited usefulness of metal coated probes. The cantilever equipped with colloid nanosphere (bio650) provided reasonable temperature stability but high signal noise, probably due to hydration of the colloidal probe, again limiting its use for mechanical transduction. Generally, the work in liquids of elevated temperatures (e.g. physiological) causes instability of the AFM laser signal reflected to the detector (Amano and Takahashi, 2013). Here, the use of non-coated probes eliminated most complications and allowed stable measurements over long time periods.

At the cellular level, temperature modulates contraction force and BR of CMs clusters; this effect can serve as an example of physiological conditions affecting heart function, conveniently studied using the developed EB-based biosensor. Data were collected for the contraction force (median of the *r*-S amplitude) and BR in the range from 26 to 37 °C (Fig. S3).

The temperature dependence showed slightly increasing values of the relative force with rising temperature, with plateau at 34 and 35 °C (88% of maximal force) and absolute maxima (quite fluctuating beating force) at the maximal temperature point. This indicates that the beating EBs are highly sensitive to temperature variation, suggesting that the constant temperature is a major factor for reliable use of the biosensor as well as it provides a great tool for arrhytmogenic drug effect detection under non standard temperature, resembling hypothermia or fever, in agreement with previously described temperature dependency in murine neonatal ventricle slices and hESC co-culture models (Pillekamp et al., 2007).

3.4. Effect of extracellular calcium level on contraction force and beat rate

Calcium is a principal mediator of the cardiac excitation-contraction coupling initiating the contraction. We then explored the effect of increased extracellular calcium concentration on EB using this biosensor set-up. The cardiac physiological concentration of Ca^{2+} range from 0.1 to 5 mM (Meli et al., 2011) while 1.8 mM is common for patch clamp and other cardiomyocyte in vitro studies (Bébarová, 2012). Real time force traces (Fig. 4A) recorded with 0.2, 1.0, 1.8, 3.6 and 5.4 mM extracellular Ca^{2+} present not only ability of the biosensor to determine the absolute contraction force (Fig. 3B) and BR (Fig. 3C) data, but also to detect and quantify irregular contractions and arrhythmias evident from traces in Fig. 4A. Such application of the biosensor enables both to detect and characterize the arrhythmias on the cellular level as well as to determine the arrhytmogenic effect of tested drugs or conditions.

Data obtained by evaluation of these curves were relativized as the absolute value for every EB sample is slightly different and therefore difficult for absolute comparison. The contraction force increased with the Ca^{2+} concentration (Fig. 4B), in agreement with well-known fact that the force of contraction is proportional to the calcium uptake in atrial and ventricular cardiomyocytes (Winegrad, 1961, Hellam and Podolsky, 1969; Katz and Lorell, 2000).

Simultaneously, BR decreased with increasing concentration of extracellular calcium (Fig. 4C). This also corresponds to the previously published non reciprocal relationship between force and BR (Burridge et al., 2014; Liu et al., 2012). Interestingly, the BR data presented higher variability for low (0.2 mM) as well as high (3.6 mM) levels of calcium, confirming dependence of coupling of excitation and contraction on calcium (Winegrad, 1961). Winegrad presented periodical drops in BR at 2.5 and 3.75 mM Ca^{2+}, almost perfectly matching our data showing uncoupling at 3.6 mM calcium (Fig. 4C). This demonstrates that the EB based biosensor can be used to study both the excitation-contraction coupling as well as to screen drugs targeted for such effects. Moreover, arrhytmogenic effect of higher calcium concentrations (3.6 and 5.4 mM) can be observed in CMG curves (Fig. 4A).

3.5. Beta-adrenergic receptors' stimulation/inhibition followed by the biosensor

The cardiomyocytes-based biosensor is not presented as purely analytical tool for measuring concentrations; its principal task is quantification of biochemical activity of the tested drugs affecting biomechanics of the cardiac syncytium. To demonstrate such application, baseline signal for different EBs was initially standardized in Tyrod buffer; afterwards, the tested compound was injected to the working chamber; the experiments included the beta-adrenergic receptor antagonist metoprolol (Beta, final concentration 70 μM), the beta-adrenergic agonist isoproterenol (1 mM) and the calcium discharger caffeine (1 mM) triggering arrhythmia (Fig. 5).

The basal physiological values of the contractile movement were characterized by R-S amplitude corresponding to force of 22.0 nN and beat rate of 67.4 per minute (bpm). In agreement with published data on beta adrenergic antagonizing activity of

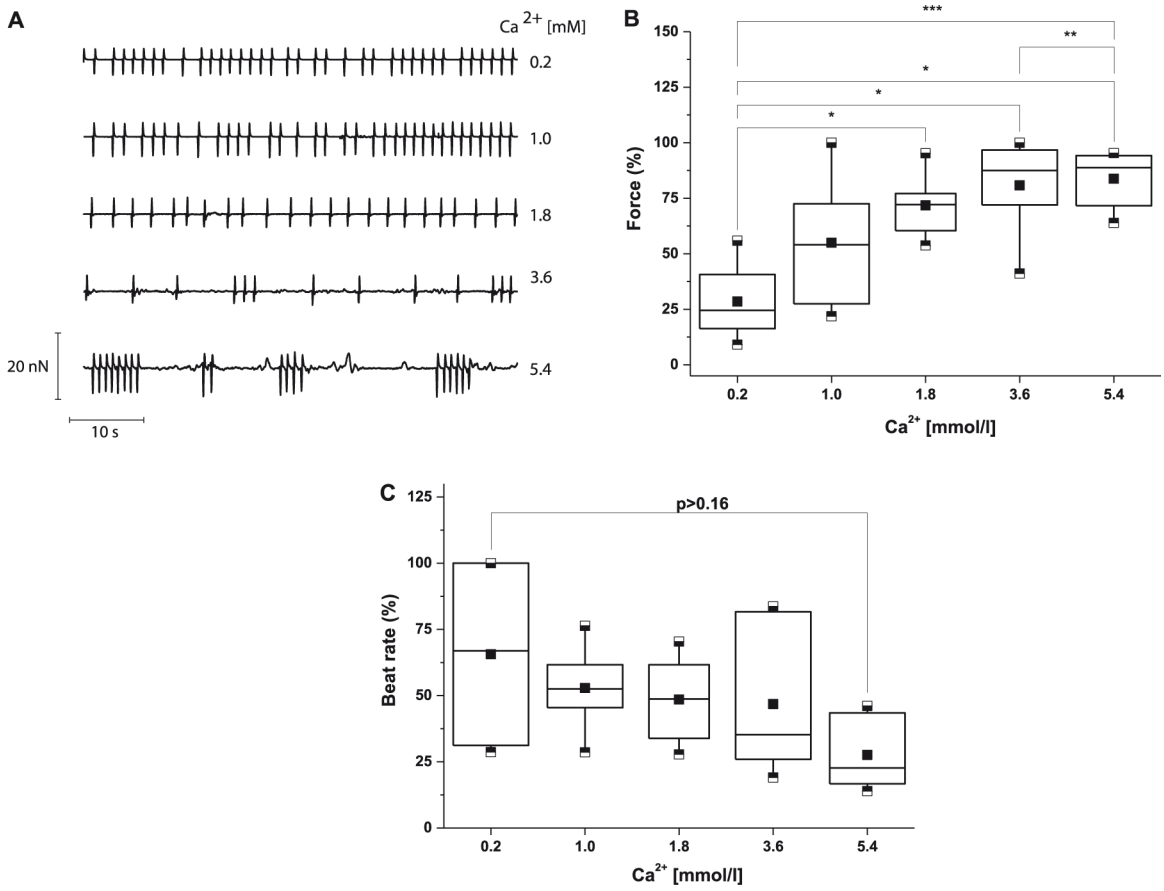

Fig. 4. Effect of calcium concentration on the beating force (*r*-S amp) and beating rate (BR) characterized by AFM microscope. Real time curves recorded in the presence of calcium concentrations indicated in the graph A. Corresponding dependencies of force (B) and beat rate (C) on the concentration of calcium. The main bars of data show middle quartile of measured data with line as median and quartiles represented by whiskers (graphs B and C). The main bars show middle quartile of the measured data with line as median and quartiles represented by whiskers (graphs B and C), N=6. Statistical significance of the data was tested by the ANOVA one way method, when the means were compared using the Bonferroni test for their significance at different levels – * $p < 0.05$,** $p < 0.01$,*** $p < 0.005$, the level of significance is indicated numerically in the graph C.

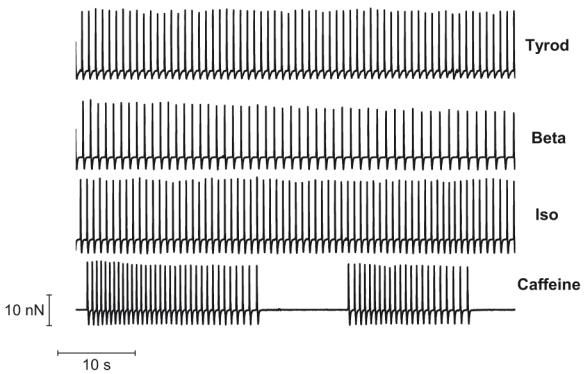

Fig. 5. Real traces of force of the beating EB measured by the AFM microscope as a response to the presence of various drugs in the measuring chamber, as indicated close to the curves.

metoprolol (Blinova et al., 2014), its addition decreased the average force down to 18.8 nN accompanied by reduction of beat rate to 53.7 bpm. On the other hand, isoproterenol (Pillekamp et al., 2012), in agreement with published data on its adrenergic stimulatory activity, induced an increase of the beat force value to 23.4 nN and beat rate to 78.8 bpm (Fig. 5).

Finally, the addition of caffeine well illustrates the ability of the biosensor to visualize very fast processes like arrhythmias. From the mathematical point of view, it is difficult to describe the arrhythmic, so called stop-and-go effect. The beating force was rather constant during the active intervals. However, the average frequency provides rather low value (58.9 bpm), it is very high (85.0 bpm) during the active period. The high deviation value stems from the irregular biological movement and not from low measurement reproducibility.

The presented data on beta adrenergic stimulation and inhibition demonstrated that the β-adrenergic signaling was mature in both hESC- and hiPSC-CMs syncytium, rendering the biosensor useful for both studying the mechanism of beta adrenergic stimulation and beta adrenergic modulatory drug screening as well as dissecting the mechanism of induced arrhythmias.

4. Conclusions

The cardiomyocytes-based embryoid body as a biorecognition element was coupled to the microcantilever probe from atomic force microscope providing micromechanical cellular biosensor. Beating force and rate of the EB contractions was transduced by AFM cantilever thus providing a robust biosensor platform suitable for whole-day testing. The cellular biosensor was optimized regarding the type of cantilever, thermostating, exchange of media and addition of tested compounds. The resulting reliable biosystem in combination with standardized protocol allowed for complex testing of compounds and conditions affecting the biomechanical properties of the embryoid body. The studied effector molecules included calcium ions, drugs as beta-blocker metoprolol

and stimulant isoprotenol, arrhythmic effects were initiated by caffeine. Furthermore, when embryoid bodies containing cardiomyocytes derived from patient's own cells via reprogrammed pluripotent stem cells are employed, the resulting biosensor can be conveniently used as the in vitro model for detailed biomechanical characterization of heart diseases such as dystrophies, including screening of novel drugs in near physiological conditions.

Conflict of interest

There is no conflict of interest.

Acknowledgments

We wish to thank Martina Vodinská and Miroslava Nehybová for their technical support, Guido Caluori from University of Genoa for reading the manuscript. We also thank Majlinda Lako from NewcastleUniversity for the cl1iPSCs line, The work has been supported by CEITEC - Central European Institute of Technology (CZ.1.05/1.1.00/02.0068 and LQ1601), FNUSA-ICRC (CZ.1.05/1.1.00/02.0123 and LQ1605) from the European Regional Development Fund and the National Program of Sustainability II., Grant Agency of the Czech Republic (P302/12/G157 and GA13-19910S). This work has also been supported by SoMoPro – Marie Curie Actions – South Moravian Region and by the European Society of Cardiology (ESC) (R12042FF).

References

Acimovic, I., Vilotic, A., Pesl, M., Lacampagne, A., Dvorak, P., Rotrekl, V., Meli, A.C., 2014. Biomed. Res. Int. 2014, 512831.
Aistrup, G.L., Shiferaw, Y., Kapur, S., Kadish, A.H., Wasserstrom, J.A., 2009. Circ. Res. 104, 639–649.
Amano, K., Takahashi, O., 2013. ArXiv1, 3053967 (Phys).
Bébarová, M., 2012. Gen. Physiol. Biophys. 31, 131–140.
Blinova, E.V., Skachilova, S.Y., Blinov, D.S., Singh, L.N., Elizarova, Y.N., Meleshkin, A.I., Ivanova, E.A., Salyamova, E.I., 2014. Vestnik aritmologii 77, 53–56.
Burridge, P.W., Metzler, S.A., Nakayama, K.H., Abilez, O.J., Simmons, C.S., Bruce, M.A., Matsuura, Y., Kim, P., Wu, J.C., Butte, M., Huang, N.F., Yang, P.C., 2014. Am. J. Transl. Res. 6, 724–735.
Chen, Y.J., Chen, Y.C., Chan, P., Lin, C.I., Chen, S.A., 2003. J. Biomed. Sci. 10, 535–543.
Dahlmann, J., Kensah, G., Kempf, H., Skvorc, D., Gawol, A., Elliott, D.A., Dräger, G., Zweigerdt, R., Martin, U., Gruh, I., 2013. Biomaterials 34, 2463–2471.
Dvorak, P., Dvorakova, D., Koskova, S., Vodinska, M., Najvirtova, M., Krekac, D., Hampl, A., 2005. Stem Cells 23, 1200–1211.
Fearn, L.A., Bartoo, M.L., Myers, J.A., Pollack, G.H., 1993. IEEE Trans. Biomed. Eng. 40, 1127–1132.
Giaever, I., Keese, C.R., 1984. Proc. Natl. Acad. Sci. USA 81, 3761–3764.
Guo, L., Abrams, R.M.C., Babiarz, J.E., Cohen, J.D., Kameoka, S., Sanders, M.J., Chiao, E., Kolaja, K.L., 2011. Toxicol. Sci. J. Soc. Toxicol. 123, 281–289.
Hane, F.T., Lee, B.Y., Petoyan, A., Rauk, A., Leonenko, Z., 2014. Biosens. Bioelectron. 54, 492–498.
Hellam, D.C., Podolsky, R.J., 1969. J. Physiol. 200, 807–819.
Holzmann, M., Nicko, A., Kühl, U., Noutsias, M., Poller, W., Hoffmann, W., Morguet, A., Witzenbichler, B., Tschöpe, C., Schultheiss, H.-P., Pauschinger, M., 2008. Circulation 118, 1722–1728.
Imamura, T., Kinugawa, K., Nitta, D., Fujino, T., Inaba, T., Maki, H., Hatano, M., Kinoshita, O., Nawata, K., Yao, A., Kyo, S., Ono, M., 2015. Int. Heart J. 56, 67–72.
International Stem Cell Initiative, Adewumi, O., Aflatoonian, B., Ahrlund-Richter, L., Amit, M., Andrews, P.W., Beighton, G., Bello, P.A., Benvenisty, N., Berry, L.S., Bevan, S., Blum, B., Brooking, J., Chen, K.G., Choo, A.B.H., Churchill, G.A., Corbel, M., Damjanov, I., Draper, J.S., Dvorak, P., Emanuelsson, K., Fleck, R.A., Ford, A., Gertow, K., Gertsenstein, M., Gokhale, P.J., Hamilton, R.S., Hampl, A., Healy, L.E., Hovatta, O., Hyllner, J., Imreh, M.P., Itskovitz-Eldor, J., Jackson, J., Johnson, J.L., Jones, M., Kee, K., King, B.L., Knowles, B.B., Lako, M., Lebrin, F., Mallon, B.S., Manning, D., Mayshar, Y., McKay, R.D.G., Michalska, A.E., Mikkola, M., Mileikovsky, M., Minger, S.L., Moore, H.D., Mummery, C.L., Nagy, A., Nakatsuji, N., O'Brien, C.M., Oh, S.K.W., Olsson, C., Otonkoski, T., Park, K.-Y., Passier, R., Patel, H., Patel, M., Pedersen, R., Pera, M.F., Piekarczyk, M.S., Pera, R.A.R., Reubinoff, B.E., Robins, A.J., Rossant, J., Rugg-Gunn, P., Schulz, T.C., Semb, H., Sherrer, E.S., Siemen, H., Stacey, G.N., Stojkovic, M., Suemori, H., Szatkiewicz, J., Turetsky, T., Tuuri, T., van den Brink, S., Vintersten, K., Vuoristo, S., Ward, D., Weaver, T.A., Young, L.A., Zhang, W., 2007. Nat. Biotechnol. 25, 803–816.
Kaneko, T., Kojima, K., Yasuda, K., 2007. Biochem Biophys. Res. Commun. 356, 494–498.
Kaneko, T., Nomura, F., Hamada, T., Abe, Y., Takamori, H., Sakakura, T., Takasuna, K., Sanbuissho, A., Hyllner, J., Sartipy, P., Yasuda, K., 2014. Sci. Rep. 4, 4670.
Katz, A.M., Lorell, B.H., 2000. Circulation 102, Iv-69-Iv-74.
Kelly, D., Mackenzie, L., Hunter, P., Smaill, B., Saint, D.A., 2006. Clin. Exp. Pharmacol. Physiol. 33, 642–648.
Krutá, M., Bálek, L., Hejnová, R., Dobšáková, Z., Eiselleová, L., Matulka, K., Bárta, T., Fojtík, P., Fajkus, J., Hampl, A., Dvořák, P., Rotrekl, V., 2013. Stem Cells 31, 693–702.
Krutá, M., Šeneklová, M., Raška, J., Salykin, A., Zerzánková, L., Pešl, M., Bártová, E., Franek, M., Baumeisterová, A., Košková, S., Neelsen, K.J., Hampl, A., Dvořák, P., Rotrekl, V., 2014. Stem Cells Dev. 23, 2443–2454.
Lavrik, N.V., Sepaniak, M.J., Datskos, P.G., 2004. Rev. Sci. Instrum. 75, 2229–2253.
Lin, W., Laitko, U., Juranka, P.F., Morris, C.E., 2007. Biophys. J. 92 (5) 1559-72.
Liu, J., Sun, N., Bruce, M.A., Wu, J.C., Butte, M.J., 2012. PLoS One 7, e37559.
Meli, A.C., Refaat, M.M., Dura, M., Reiken, S., Wronska, A., Wojciak, J., Carroll, J., Scheinman, M.M., Marks, A.R., 2011. Circ. Res. 22 109(3):281–90.
Mummery, C., Ward, D., Van den Brink, C.E., Bird, S.D., Doevendans, P.A., Opthof, T., La Riviere, D., Brutel, A., Tertoolen, L., Van Der Heyden, M., 2002. (others). J. Anat. 200, 233–242.
Neagoe, C., Opitz, C.A., Makarenko, I., Linke, W.A., 2003. J. Muscle Res. Cell Motil. 24, 175–189.
Obataya, I., Nakamura, C., Han, S., Nakamura, N., Miyake, J., 2005. Biosens. Bioelectron. 20, 1652–1655.
Pesl, M., Acimovic, I., Pribyl, J., Hezova, R., Vilotic, A., Fauconnier, J., Vrbsky, J., Kruzliak, P., Skladal, P., Kara, T., Rotrekl, V., Lacampagne, A., Dvorak, P., Meli, A.C., 2014. Heart Vessel. 29, 834–846.
Pilkerton, C.S., Singh, S.S., Bias, T.K., Frisbee, S.J., 2015. J. Am. Heart Assoc. 4, e001650.
Pillekamp, F., Reppel, M., Rubenchyk, O., Pfannkuche, K., Matzkies, M., Bloch, W., Sreeram, N., Brockmeier, K., Hescheler, J., 2007. Stem Cells Dayt. Ohio 25, 174–180.
Pillekamp, F., Haustein, M., Khalil, M., Emmelheinz, M., Nazzal, R., Adelmann, R., Nguemo, F., Rubenchyk, O., Pfannkuche, K., Matzkies, M., Reppel, M., Bloch, W., Brockmeier, K., Hescheler, J., 2012. Stem Cells Dev. 21, 2111–2121.
Rodriguez, A.G., Han, S.J., Regnier, M., Sniadecki, N.J., 2011. Biophys. J. 101, 2455–2464.
Rodriguez, M.L., Graham, B.T., Pabon, L.M., Han, S.J., Murry, C.E., Sniadecki, N.J., 2014. J. Biomech. Eng. 136, 051005.
Samori, P., 2009. STM and AFM Studies on (Bio) molecular Systems: Unravelling the Nanoworld. Springer Science & Business Media,, Germany.
Sondergaard, C.S., Mathews, G., Wang, L., Jeffreys, A., Sahota, A., Wood, M., Ripplinger, C.M., Si, M.-S., 2012. Ann. Thorac. Surg. 94, 1241–1249.
Stienen, G.J.M., 2015. J. Muscle Res. Cell Motil. 36, 47–60.
Sundararajan, S., Bhushan, B., 2002. Sens. Actuators Phys. 101, 338–351.
Takahashi, K., Tanabe, K., Ohnuki, M., Narita, M., Ichisaka, T., Tomoda, K., Yamanaka, S., 2007. Cell 131, 861–872.
Thompson, S.A., Copeland, C.R., Reich, D.H., Tung, L., 2011. Circulation 123, 2083–2093.
Thomson, J.A., Itskovitz-Eldor, J., Shapiro, S.S., Waknitz, M.A., Swiergiel, J.J., Marshall, V.S., Jones, J.M., 1998. Science 282, 1145–1147.
Vahabi, S., Nazemi Salman, B., Javanmard, A., 2013. Iran. J. Med. Sci. 38, 76–83.
Wang, C., Kim, J., Zhu, Y., Yang, J., Lee, G.-H., Lee, S., Yu, J., Pei, R., Liu, G., Nuckolls, C., Hone, J., Lin, Q., 2015. Biosens. Bioelectron. 71, 222–229.
Wang, J., Wan, Z., Liu, W., Li, L., Ren, L., Wang, X., Sun, P., Ren, L., Zhao, H., Tu, Q., Zhang, Z., Song, N., Zhang, L., 2009. Biosens. Bioelectron. 25, 721–727.
Winegrad, S., 1961. Circullation 24, 523.
Yamazaki, T., Komuro, I., Yazaki, Y., 1998. Cell. Signalling 10, 693–698.
Zhang, L., Yang, F., Cai, J.-Y., Yang, P.-H., Liang, Z.-H., 2014. Biosens. Bioelectron. 56, 271–277.